

Giant magnetic-field dependence of the coupling between spin Tomonaga-Luttinger liquids in $\text{BaCo}_2\text{V}_2\text{O}_8$

M. Klanjšek,^{1,2,*} M. Horvatić,² S. Krämer,² S. Mukhopadhyay,² H. Mayaffre,²
C. Berthier,² E. Canévet,³ B. Grenier,⁴ P. Lejay,⁵ and E. Orignac⁶

¹Jožef Stefan Institute, Jamova 39, and EN-FIST Centre of Excellence, Dunajska 156, 1000 Ljubljana, Slovenia

²Laboratoire National des Champs Magnétiques Intenses - CNRS, UJF, UPS and INSA, 38042 Grenoble, France

³Institut Laue-Langevin, 38042 Grenoble, France

⁴CEA, INAC-SPSMS and Univ. Grenoble Alpes, 38054 Grenoble, France

⁵Institut Néel - CNRS and UJF, 38042 Grenoble, France

⁶LPENSL - CNRS, UMR 5672, 69364 Lyon, France

(Dated: April 16, 2021)

We use nuclear magnetic resonance to map the complete low-temperature phase diagram of the antiferromagnetic Ising-like spin-chain system $\text{BaCo}_2\text{V}_2\text{O}_8$ as a function of the magnetic field applied along the chains. In contrast to the predicted crossover from the longitudinal incommensurate phase to the transverse antiferromagnetic phase, we find a sequence of three magnetically ordered phases between the critical fields 3.8 T and 22.8 T. Their origin is traced to the giant magnetic-field dependence of the total effective coupling between spin chains, extracted to vary by a factor of 24. We explain this novel phenomenon as emerging from the combination of nontrivially coupled spin chains and incommensurate spin fluctuations in the chains treated as Tomonaga-Luttinger liquids.

PACS numbers: 75.10.Pq, 75.30.Kz, 71.10.Pm, 76.60.-k

The study of emergent phenomena in interacting quantum systems is at the heart of condensed-matter physics. Interacting fermions confined to one dimension (1D) emerge in a quantum-critical state with non-particle-like excitations, whose low-energy description is known as the Tomonaga-Luttinger liquid (TLL) [1]. As any correlation function adopts a universal form, insensitive to the microscopic details, the TLL description applies to a wide range of systems, like 1D metals [2], edge states of quantum Hall effect [3], quantum wires [4], carbon nanotubes [5] and 1D arrays of atoms on surfaces [6] or in optical traps [7]. The simplest and experimentally most accessible TLLs are realized in 1D quantum antiferromagnets hosting spin chains or ladders, which can be mapped onto interacting spinless fermions [8]. In particular, two spin-ladder systems, $(\text{C}_5\text{H}_{12}\text{N})_2\text{CuBr}_4$ (BPCB) [9–13] and $(\text{C}_7\text{H}_{10}\text{N})_2\text{CuBr}_4$ (DIMPY) [14–19], allowed to confirm the predicted correlation functions not only in form, but also quantitatively as a function of the magnetic field, which controls the Fermi level [1].

While isolated TLLs cannot order because of strong quantum fluctuations, a weak coupling between TLLs leads at low temperatures to the 3D ordered state, which inherits the properties of the dominant fluctuation mode. As the Fermi surface in a TLL is reduced to two points, k_F and $-k_F$, fermionic fluctuations can only occur at the wavevectors $q = 0$ and $q = 2k_F$ [1]. In antiferromagnetic spin chains or ladders in a magnetic field, the corresponding spin fluctuations are transverse (i.e., involving spin components perpendicular to the field) *antiferromagnetic*, at the antiferromagnetically shifted wavevector $q = \pi$, and longitudinal (i.e., involving spin components along the field) *incommensurate* at the incommensurate

wavevector $q = 2k_F$, respectively [1]. For the Heisenberg exchange between spins, the transverse fluctuations dominate and a weakly coupled system develops a transverse antiferromagnetic order at low temperatures [20, 21], in the gapless region between the critical fields B_c and B_s , which correspond to the edges of the fermion band. Examples include BPCB [10, 22], DIMPY [16], F_5PNN [23] and copper nitrate [24]. More interestingly, for the Ising-like exchange between spins and the field directed along the exchange anisotropy axis, the transverse fluctuations dominate only in the high-field region, while in the low-field region the longitudinal fluctuations dominate. Accordingly, the low-temperature ordered state in a weakly coupled system is expected to switch from the longitudinal incommensurate to the transverse antiferromagnetic as the field is increased from B_c to B_s [25]. An experimental confirmation of this important prediction reflecting the essence of the TLL description is still missing.

Realizations of the archetypal Ising-like (i.e., XXZ) antiferromagnetic spin-1/2 chain model in the longitudinal field [26] are therefore highly desired but unfortunately rare. Among them, $\text{BaCo}_2\text{V}_2\text{O}_8$ [27] has been recently studied [28–41] as one of a few with accessible critical fields, i.e., $B_c = 3.8$ T and $B_s = 22.8$ T [30]. The system develops a standard low-temperature Néel ordered phase in the field range up to B_c [29, 31] (Fig. 1). Above B_c , an exotic low-temperature incommensurate phase extending up to ~ 9 T was identified [31, 32, 37] (Fig. 1), confirming the first part of the prediction [25]. We continue the exploration of the phase diagram up to B_s and find a sequence of *three* ordered phases above B_c , in striking contrast to the predicted crossover between the *two* phases. Surprisingly, all three ordered phases appear to

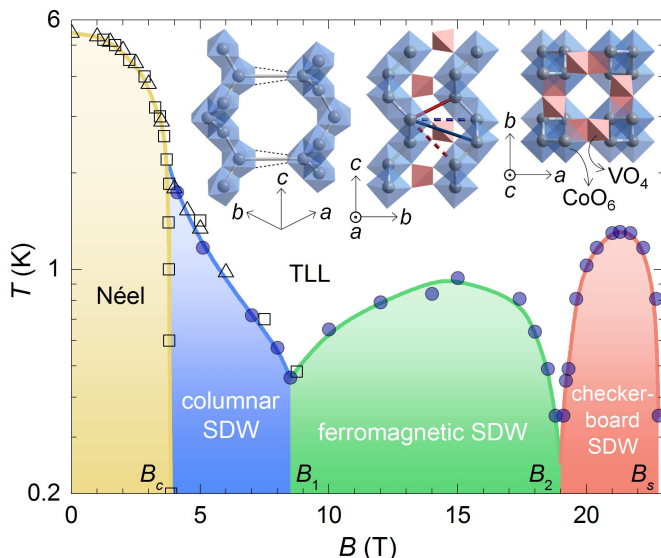


FIG. 1: (color online) Phase diagram of $\text{BaCo}_2\text{V}_2\text{O}_8$ as a function of temperature T and the magnetic field B applied along the c axis. Phase boundaries are obtained from the T_1^{-1} data displayed in Figs. 2(a,b) (circles) and from the specific heat (squares) and neutron diffraction data (triangles) in Ref. [37]. Lines are guides to the eye. Inset shows three views of the structural unit of $\text{BaCo}_2\text{V}_2\text{O}_8$. Edge-sharing CoO_6 octahedra (blue) form chains along c . Exchange coupling between spin-1/2 Co^{2+} ions (grey spheres) in neighboring chains is mediated by O_4 plaquettes (thin dashed lines) for NNN chains (neighbors along the a - b bisectors) and by VO_4 tetrahedra (red) for NN chains (neighbors along a or b). The intrachain coupling mediated by shorter O_2 bridges is much stronger. Thick lines represent different types of interchain couplings.

be determined by incommensurate spin fluctuations. We show that these fluctuations combined with nontrivially coupled nearest-neighboring (NN) spin chains lead to a remarkably huge field dependence of the effective coupling between the NN chains, matching the experimental result obtained from the phase boundary. The three ordered phases then result from the competition between this variable coupling and the fixed coupling between the next-nearest-neighboring (NNN) chains, in close analogy to the frustrated spin-1/2 model on a square lattice [42]. This novel phenomenon is thus emergent in nature: although the couplings between individual spins are field-independent, the collective coupling between the 1D spin arrangements is strongly field-dependent.

In our ^{51}V nuclear magnetic resonance (NMR) experiments, a single crystal of $\text{BaCo}_2\text{V}_2\text{O}_8$ [33] was oriented with its c axis, coinciding with the exchange anisotropy axis, accurately along the field direction. The phase boundary in Fig. 1 was mapped by means of the NMR relaxation rate T_1^{-1} , which directly probes the low-energy spin fluctuations [43]. The temperature and field dependence of T_1^{-1} measured at selected field and temperature values are shown in Figs. 2(a) and (b), respectively.

The datasets reveal a clear second-order phase transition through the characteristic peak indicative of the critical spin fluctuations. The transition point marks the onset of a strong T_1^{-1} decrease on decreasing temperature, reflecting the suppression of spin fluctuations in the ordered phase [44]. In the $T_1^{-1}(T)$ datasets taken between 8 and 14 T, the transition peak is smeared out, most likely because of the less accurate sample orientation in the cryostat used below 14 T, but can still be defined as the onset of the $T_1^{-1}(T)$ decrease. The overall phase boundary outlines two new ordered phases between $B_1 = 8.6$ T and B_s , and the first question is what is their nature.

Figs. 2(c-f) show representative NMR spectra in various phases. The crystal structure of $\text{BaCo}_2\text{V}_2\text{O}_8$ [27] contains parallel chains of magnetic Co^{2+} ions running along c and forming a square lattice in the tetragonal a - b plane (Fig. 1 inset). Above the phase boundary, throughout the TLL phase (Fig. 1), the NMR spectrum exhibits a single peak [Fig. 2(c)] generated by a single crystallographic V site, which is located between the NN chains. The appearance of the incommensurate order, where static spin-density waves (SDWs) form in chains, leads to the characteristic U-shaped broadening [45]. In the ordered phase between B_c and B_1 , the spectrum actually develops two such U-shaped components of equal area [Fig. 2(d)]. This is consistent with the *columnar* nature of the incommensurate phase in this field range, as observed by neutron diffraction, where the symmetry between a and b directions is broken, so that the SDWs are in phase (in opposite phase) along one (the other) direction [37]. In the ordered phase above B_1 , the NMR spectrum exhibits a single broad peak with pronounced wings. A single U-shaped component is revealed after a longer NMR echo decay time [Figs. 2(e,f)], showing that the symmetry between a and b directions is restored. Together with the simulation of the spectral splitting [46], this suggests a *ferromagnetic* nature of the incommensurate phase, meaning that all SDWs are in phase. The origin of the central narrow component observed at short echo decay times is unclear at the moment. For instance, a distribution corresponding to a long-wavelength 2D sinusoidal modulation of the SDW amplitude in the a - b plane perfectly reproduces the lineshape [Fig. 2(e)]. Alternatively, a narrow central component may also come from an eventual presence of the transverse antiferromagnetic phase coexisting with the longitudinal incommensurate phase [46]. Both scenarios require additional terms in the XXZ chain Hamiltonian, which is a topic for further studies. The NMR spectrum remains qualitatively unchanged up to B_s and does not offer insight into the remaining transition at $B_2 = 19$ T.

For further insight into the nature of the ordered phases, we show that the behavior of $T_1^{-1}(T)$ above the phase boundary is quantitatively consistent with the TLL prediction for the longitudinal incommensurate fluctuations. A power-law dependence $T_1^{-1} \propto u^{-1/\eta} T^{1/\eta-1}$ is

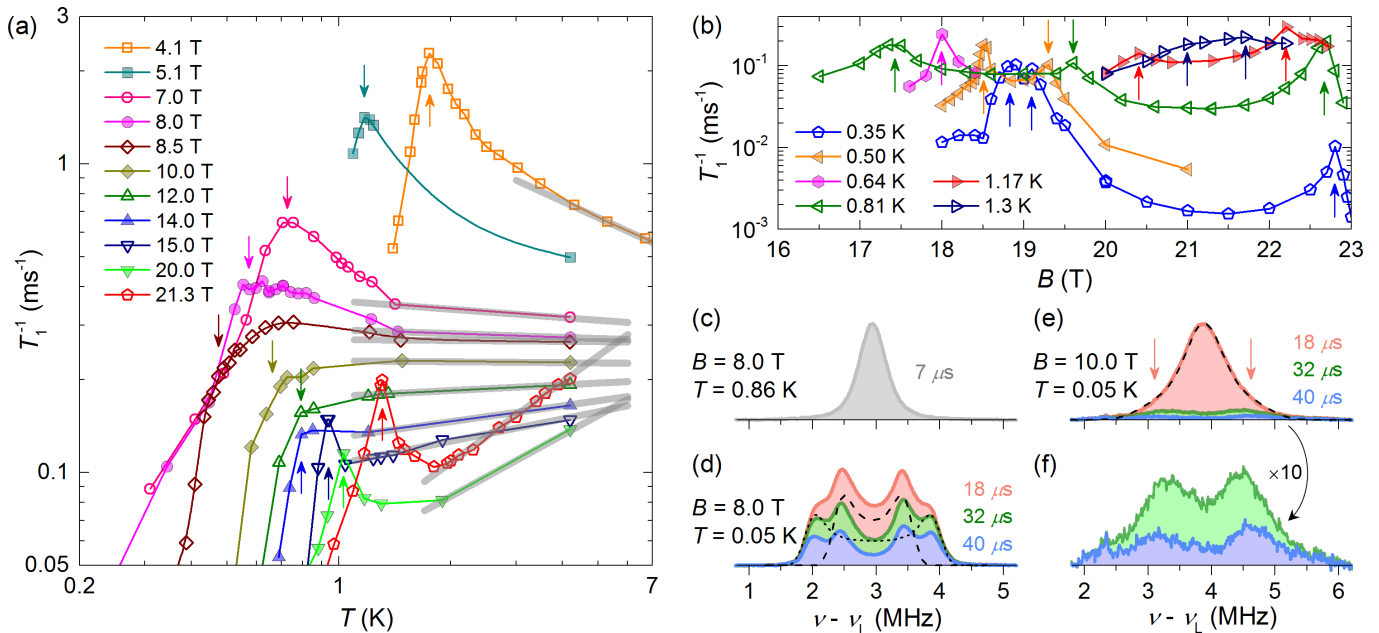


FIG. 2: (color online) (a) Temperature dependence of T_1^{-1} in $\text{BaCo}_2\text{V}_2\text{O}_8$ for different magnetic fields B applied along the c axis. Thin lines are guides to the eye. Arrows mark the extracted temperatures T_c of the transition from the TLL phase to the ordered phase. Thick gray lines are power-law fits in the TLL phase. (b) Field dependence of T_1^{-1} for different temperatures T , with the presentation as in (a). (c-f) Representative ^{51}V NMR spectra of various phases recorded after different NMR echo decay times. The frequency scale is relative to $\nu_L = \gamma B$ where $\gamma = 11.193$ MHz/T and B is corrected for demagnetizing effect. (c) In the TLL phase, the spectrum exhibits a single peak. (d) In the columnar SDW phase, the spectrum is reproduced by two U-shaped components of the same area. They are generated by two sets of V sites located between the NN chains hosting SDWs that are either in phase (dashed line) or in opposite phase (dotted line). (e) In the ferromagnetic SDW phase, the spectrum can be reproduced by a distribution of U-shaped components generated by a single set of V sites (dashed line). A distribution based on the 2D sinusoidal modulation of the SDW amplitude in the a - b plane results in a spectrum with a large central weight and pronounced wings (indicated by arrows). (f) Spectra from (e) scaled up 10-times.

expected for this fluctuation mode, where η is the interaction exponent and u is the velocity of spin excitations (in kelvin units). This is obtained from the corresponding expression for the transverse antiferromagnetic fluctuations [10] by replacing η with $1/\eta$ [25]. The $T_1^{-1}(T)$ dataset at 21.3 T clearly exhibits the predicted power-law behavior, but the experimental limitations allowed us to take only a small number of data points in other datasets [Fig. 2(a)]. Nevertheless, η is determined simply from the $T_1^{-1}(T)$ slope (in a log-log scale), which exhibits a significant variation over the datasets. Moreover, once η is known, the knowledge of the NMR form factor [46] allows us to determine u from the prefactor to the power-law behavior of $T_1^{-1}(T)$ datasets, which spreads over a decade. Despite sparse datasets, we can thus estimate the field dependence of the TLL parameters η and u quite accurately. They are shown in Figs. 3(a,b) together with the theoretical prediction for the spin-1/2 XXZ chain model as applied to $\text{BaCo}_2\text{V}_2\text{O}_8$ [25], and the agreement is excellent. This empirically shows a negligible sensitivity of T_1^{-1} to the antiferromagnetic spin fluctuations, which would yield power-law slopes of the opposite sign, i.e., $\eta - 1$ instead of $1/\eta - 1$ (e.g., -0.5 instead of 1 at B_s where $\eta = 1/2$) [47]. Even more, as the change of spin dy-

namics upon transition is seen by T_1^{-1} [Fig. 2(a)], which is thus sensitive mainly to the incommensurate spin fluctuations, this fluctuation mode appears to condense in the ordered phase in the *whole* range from B_c to B_s .

An unexpected dominance of the incommensurate mode for the nature of the ordered phases, even in the high-field region, originates from the strong enhancement of the associated total effective interchain coupling J' towards B_s . A huge spread of the $T_1^{-1}(T)$ datasets in the TLL phase [Fig. 2(a)] already *qualitatively* points to such an enhancement. To see how, we recall that T_1^{-1} is proportional to the imaginary part of the local dynamical spin susceptibility χ [43]. For a system of weakly-coupled spin chains, each having the susceptibility χ_{1D} , we can write $\chi = \chi_{1D}/(1 - J'\chi_{1D})$ in the random-phase approximation (RPA). The $T_1^{-1}(T)$ peak at the transition point T_c then translates to $J' = 1/\chi_{1D}(T_c)$, where $\chi_{1D}(T_c)$ is related to $T_{1c}^{-1} = T_1^{-1}(T_c)$ in the absence of critical fluctuations, i.e., extrapolated to T_c from the TLL power-law behavior. The total variation $J'(20 \text{ T})/J'(4.1 \text{ T})$ can then be approximated by $T_{1c}^{-1}(20 \text{ T})/T_{1c}^{-1}(4.1 \text{ T}) \approx 20$, a surprisingly high factor. In contrast, the same approximate procedure applied to other known spin chain or ladder systems, e.g., DIMPY [18], leads to an almost field-

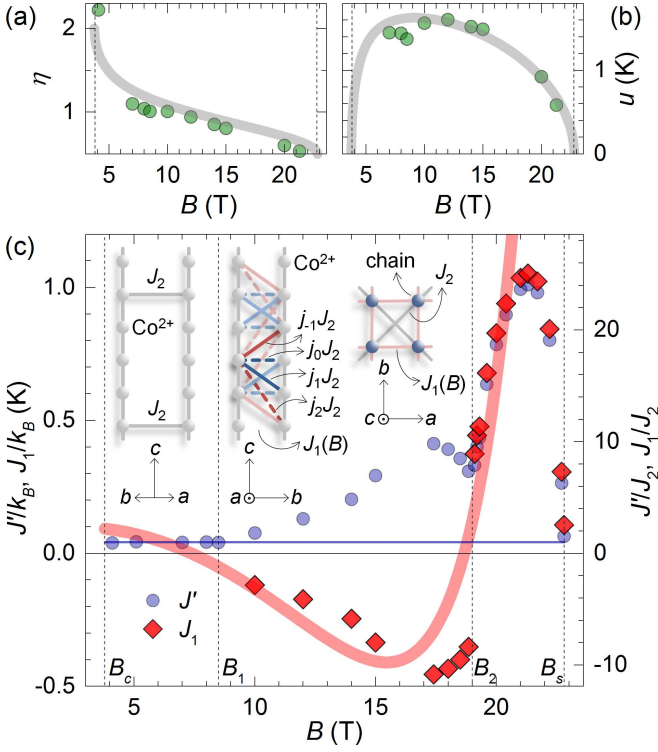


FIG. 3: (color online) (a,b) Dependence of the TLL parameters η and u on the magnetic field B in $\text{BaCo}_2\text{V}_2\text{O}_8$ as extracted from the power-law fits in Fig. 2(a). Thick gray lines are predictions of the spin-1/2 XXZ chain model with parameters relevant to $\text{BaCo}_2\text{V}_2\text{O}_8$ [25]. (c) Magnetic-field dependence of the effective interchain exchange coupling J' (circles) and of the exchange coupling J_1 (diamonds) between the NN chains as extracted from the phase boundary in Fig. 1. Thin blue line is a constant fit to the $J'(B)$ data between B_s and B_1 giving $J_2/k_B = 0.042$ K. Thick red line is a fit to the $J_1(B)$ data above B_1 using Eq. (2). Inset shows the proposed schemes of interchain exchange couplings corresponding respectively to the structural units in the inset of Fig. 1.

independent J' . We can extract $J'(B)$ in $\text{BaCo}_2\text{V}_2\text{O}_8$ also *quantitatively* from the phase boundary $T_c(B)$ between B_c and B_s using the RPA expression evaluated for the longitudinal incommensurate spin fluctuations [25]:

$$T_c = \frac{u}{2\pi} \left[\frac{\Delta J' A_z}{k_B u} \sin\left(\frac{\pi}{2\eta}\right) B^2 \left(\frac{1}{4\eta}, 1 - \frac{1}{2\eta} \right) \right]^{\eta/(2\eta-1)}, \quad (1)$$

where $A_z(B)$ is a known amplitude of the longitudinal fluctuations [48], Δ the exchange anisotropy, k_B the Boltzmann constant and $B^2(x, y)$ the square of the beta function. The resulting $J'(B)/k_B$ shown in Fig. 3(c) amounts to 0.042 K up to B_1 , and exhibits a giant variation by a factor of $1 \text{ K}/0.042 \text{ K} = 24$ above B_1 .

Finally, we show that the crucial ingredient leading to the extracted giant $J'(B)$ dependence is a nontrivial, zigzag-like pattern of individual antiferromagnetic couplings between the NN chains [Fig. 3(c) inset], all running along VO_4 tetrahedra (Fig. 1 inset). If we parametrize

them by the weights j_{-1} , j_0 , j_1 and j_2 relative to the individual antiferromagnetic coupling J_2 between the NNN chains [Fig. 3(c) inset], the whole pattern consisting of 4 groups of 4 identical couplings within a helical chain period (containing 4 chain units) sums up to

$$J_1 = 4J_2 \left[j_0 + (j_{-1} + j_1) \cos q + j_2 \cos(2q) \right] \quad (2)$$

in the presence of spin fluctuations with the wavevector q . Namely, each coupling “tilted” by p chain units simply picks the corresponding phase shift pq . For incommensurate fluctuations with $q = 2k_F$, the field dependence of J_1 comes from the relation $2k_F(B) = \pi[1 - 2m_z(B)]$ where $m_z(B)$ is the field-induced magnetization [25]. To go further, we realize that $J_1(B)$ and J_2 couplings in the a - b plane [Fig. 3(c) inset] outline a pattern equivalent to the J_1 - J_2 model on a square lattice [42]. Depending on the ratio J_1/J_2 , this model realizes one of the three phases, each one exhibiting a different total effective coupling J' : columnar for $|J_1| < 2J_2$ where $J' = J_2$, ferromagnetic for $J_1 < -2J_2$ where $J' = -J_1 - J_2$ and checkerboard for $J_1 > 2J_2$ where $J' = J_1 - J_2$ [42]. Applying these expressions to $\text{BaCo}_2\text{V}_2\text{O}_8$, a field-independent J' in the columnar phase (between B_c and B_1) immediately leads to $J_2/k_B = 0.042$ K. In the ferromagnetic phase (between B_1 and B_2) we can then extract $J_1(B) = -J'(B) - J_2$. Finally, the phase between B_2 and B_s should be checkerboard, hence $J_1(B) = J'(B) + J_2$. Accordingly reconstructed $J_1(B)$ dataset is shown in Fig. 3(c) together with the fit using Eq. (2) with $j_0 = 8.9$, $j_{-1} + j_1 = 15.5$, $j_2 = 7.1$ and known $m_z(B)$ [31]. The fit fails to reproduce the $J_1(B)$ data points only close to the critical field B_s where the TLL description is expected to fail anyway [1]. The obtained $J_1(B)$ reaches two orders of magnitude over J_2 and exhibits a remarkable sign change (to ferromagnetic), although all the individual couplings between the NN chains are antiferromagnetic. In contrast, for transverse antiferromagnetic fluctuations we set $q = \pi$ in Eq. (2), leading to a field-independent J_1 , which is only of the order of J_2 . This is the reason why the transverse antiferromagnetic order is not realized. The overall quantitative account of the $J_1(B)$ dependence a posteriori supports the previously obtained hint at the incommensurate order in the whole range between B_c and B_s .

To conclude, our study identifies a hugely field-dependent effective magnetic coupling between spin chains in $\text{BaCo}_2\text{V}_2\text{O}_8$ as a new phenomenon emerging from the incommensurate fluctuations in TLLs coupled in a zigzag-like manner. This phenomenon could be realized also in other spin chain or ladder systems meeting the two conditions necessary for the dominance of the incommensurate fluctuations, i.e., anisotropy of the involved $S = 1/2$ spins [30] and the zigzag-like couplings. It is important to be aware of this possibility, as it may lead to a complicated phase diagram where a simple one would be expected. This may be the case in the

recently studied BiCu_2PO_6 , which satisfies both conditions [49, 50] and exhibits a rich phase diagram [51]. The phenomenon could also be used deliberately as a source of tunable coupling between TLLs. For instance, implemented in an array of quantum wires, it would allow to control the current perpendicular to the wires, including its sign, simply by the gate voltage applied to the wires.

The work was partly supported by the Slovenian ARRS project No. J1-2118 and by the French ANR project NEMSIKOM. The high-field part of this work was supported by EuroMagNET under the EU contract number 228043. LNCMI is a member of the European Magnetic Field Laboratory (EMFL).

* Electronic address: martin.klanjsek@ijs.si

- [1] T. Giamarchi, *Quantum Physics in One Dimension* (Oxford Univ. Press, Oxford, 2004).
- [2] A. Schwartz, M. Dressel, G. Grüner, V. Vescoli, L. Degiorgi, and T. Giamarchi, *Phys. Rev. B* **58**, 1261 (1998).
- [3] M. Grayson, D. C. Tsui, L. N. Pfeiffer, K. W. West, and A. M. Chang, *Phys. Rev. Lett.* **80**, 1062 (1998).
- [4] Y. Jompol, C. J. B. Ford, J. P. Griffiths, I. Farrer, G. A. C. Jones, D. Anderson, D. A. Ritchie, T. W. Silk, and A. J. Schofield, *Science* **325**, 597 (2009).
- [5] H. Ishii, H. Kataura, H. Shiozawa, H. Yoshioka, H. Otsubo, Y. Takayama, T. Miyahara, S. Suzuki, Y. Achiba, M. Nakatake, T. Narimura, M. Higashiguchi, K. Shimada, H. Namatame, and M. Taniguchi, *Nature* **426**, 540 (2003).
- [6] C. Blumenstein, J. Schäfer, S. Mietke, S. Meyer, A. Dollinger, M. Lochner, X. Y. Cui, L. Patthey, R. Matzdorf, and R. Claessen, *Nature Phys.* **7**, 776 (2011).
- [7] A. Vogler, R. Labouvie, G. Barontini, S. Eggert, V. Guarnera, and H. Ott, *Phys. Rev. Lett.* **113**, 215301 (2014).
- [8] F. D. M. Haldane, *Phys. Rev. Lett.* **45**, 1358 (1980).
- [9] T. Lorenz, O. Heyer, M. Garst, F. Anfuso, A. Rosch, Ch. Rüegg, and K. Krämer, *Phys. Rev. Lett.* **100**, 067208 (2008).
- [10] M. Klanjšek, H. Mayaffre, C. Berthier, M. Horvatić, B. Chiari, O. Piovesana, P. Bouillot, C. Kollath, E. Orignac, R. Citro, and T. Giamarchi, *Phys. Rev. Lett.* **101**, 137207 (2008).
- [11] B. Thielemann, Ch. Rüegg, H. M. Rønnow, A. M. Läuchli, J.-S. Caux, B. Normand, D. Biner, K. W. Krämer, H.-U. Güdel, J. Stahn, K. Habicht, K. Kiefer, M. Boehm, D. F. McMorrow, and J. Mesot, *Phys. Rev. Lett.* **102**, 107204 (2009).
- [12] B. Thielemann, Ch. Rüegg, K. Kiefer, H. M. Rønnow, B. Normand, P. Bouillot, C. Kollath, E. Orignac, R. Citro, T. Giamarchi, A. M. Läuchli, D. Biner, K. W. Krämer, F. Wolff-Fabris, V. S. Zapf, M. Jaime, J. Stahn, N. B. Christensen, B. Grenier, D. F. McMorrow, and J. Mesot, *Phys. Rev. B* **79**, 020408 (2009).
- [13] P. Bouillot, C. Kollath, A. M. Läuchli, M. Zvonarev, B. Thielemann, C. Rüegg, E. Orignac, R. Citro, M. Klanjšek, C. Berthier, M. Horvatić, and T. Giamarchi, *Phys. Rev. B* **83**, 054407 (2011).
- [14] T. Hong, Y. H. Kim, C. Hotta, Y. Takano, G. Tremelling, M. M. Turnbull, C. P. Landee, H.-J. Kang, N. B. Christensen, K. Lefmann, K. P. Schmidt, G. S. Uhrig, and C. Broholm, *Phys. Rev. Lett.* **105**, 137207 (2010).
- [15] K. Ninios, T. Hong, T. Manabe, C. Hotta, S. N. Herrer, M. M. Turnbull, C. P. Landee, Y. Takano, and H. B. Chan, *Phys. Rev. Lett.* **108**, 097201 (2012).
- [16] D. Schmidiger, P. Bouillot, S. Mühlbauer, S. Gvasaliya, C. Kollath, T. Giamarchi, and A. Zheludev, *Phys. Rev. Lett.* **108**, 167201 (2012).
- [17] D. Schmidiger, P. Bouillot, T. Guidi, R. Bewley, C. Kollath, T. Giamarchi, and A. Zheludev, *Phys. Rev. Lett.* **111**, 107202 (2013).
- [18] M. Jeong, H. Mayaffre, C. Berthier, D. Schmidiger, A. Zheludev, and M. Horvatić, *Phys. Rev. Lett.* **111**, 106404 (2013).
- [19] K. Yu. Povarov, D. Schmidiger, N. Reynolds, A. Zheludev, R. Bewley, arXiv: 1406.6876 (2014).
- [20] T. Giamarchi and A. M. Tsvelik, *Phys. Rev. B* **59**, 11398 (1999).
- [21] S. Wessel and S. Haas, *Phys. Rev. B* **62**, 316 (2000).
- [22] C. Rüegg, K. Kiefer, B. Thielemann, D. F. McMorrow, V. Zapf, B. Normand, M. B. Zvonarev, P. Bouillot, C. Kollath, T. Giamarchi, S. Capponi, D. Poilblanc, D. Biner, and K. W. Krämer, *Phys. Rev. Lett.* **101**, 247202 (2008).
- [23] Y. Yoshida, N. Tateiwa, M. Mito, T. Kawae, K. Takeda, Y. Hosokoshi, and K. Inoue, *Phys. Rev. Lett.* **94**, 037203 (2005).
- [24] B. Willenberg, H. Ryll, K. Kiefer, D. A. Tennant, F. Groitl, K. Rolfs, P. Manuel, D. Khalavayin, K. C. Rule, A. U. B. Wolter, S. Süllow, arXiv: 1406.6149 (2014).
- [25] K. Okunishi and T. Suzuki, *Phys. Rev. B* **76**, 224411 (2007).
- [26] C. N. Yang and C. P. Yang, *Phys. Rev.* **150**, 321 (1966).
- [27] R. Wichmann and Hk. Müller-Buschbaum, *Z. anorg. allg. Chem.* **534**, 153 (1986).
- [28] Z. He, D. Fu, T. Kyōmen, T. Taniyama, and M. Itoh, *Chem. Mater.* **17**, 2924 (2005).
- [29] Z. He, T. Taniyama, T. Kyōmen, and M. Itoh, *Phys. Rev. B* **72**, 172403 (2005).
- [30] S. Kimura, H. Yashiro, K. Okunishi, M. Hagiwara, Z. He, K. Kindo, T. Taniyama, and M. Itoh, *Phys. Rev. Lett.* **99**, 087602 (2007).
- [31] S. Kimura, T. Takeuchi, K. Okunishi, M. Hagiwara, Z. He, K. Kindo, T. Taniyama, and M. Itoh, *Phys. Rev. Lett.* **100**, 057202 (2008).
- [32] S. Kimura, M. Matsuda, T. Masuda, S. Hondo, K. Kaneko, N. Metoki, M. Hagiwara, T. Takeuchi, K. Okunishi, Z. He, K. Kindo, T. Taniyama, and M. Itoh, *Phys. Rev. Lett.* **101**, 207201 (2008).
- [33] P. Lejay, E. Canevet, S. K. Srivastava, B. Grenier, M. Klanjšek, and C. Berthier, *J. Cryst. Growth* **317**, 128 (2011).
- [34] Y. Kawasaki, J. L. Gavilano, L. Keller, J. Schefer, N. B. Christensen, A. Amato, T. Ohno, Y. Kishimoto, Z. He, Y. Ueda, and M. Itoh, *Phys. Rev. B* **83**, 064421 (2011).
- [35] Z. Y. Zhao, X. G. Liu, Z. He, X. M. Wang, C. Fan, W. P. Ke, Q. J. Li, L. M. Chen, X. Zhao, and X. F. Sun, *Phys. Rev. B* **85**, 134412 (2012).
- [36] Y. Ideta, Y. Kawasaki, Y. Kishimoto, T. Ohno, Y. Michihiro, Z. He, Y. Ueda, and M. Itoh, *Phys. Rev. B* **86**, 094433 (2012).
- [37] E. Canévet, B. Grenier, M. Klanjšek, C. Berthier,

- M. Horvatić, V. Simonet, and P. Lejay, Phys. Rev. B **87**, 054408 (2013).
- [38] S. Kimura, K. Okunishi, M. Hagiwara, K. Kindo, Z. He, T. Taniyama, M. Itoh, K. Koyama, and K. Watanabe, J. Phys. Soc. Jpn. **82**, 033706 (2013).
- [39] S. K. Niesen, G. Kolland, M. Seher, O. Breunig, M. Valldor, M. Braden, B. Grenier, and T. Lorenz, Phys. Rev. B **87**, 224413 (2013).
- [40] S. K. Niesen, O. Breunig, S. Salm, M. Seher, M. Valldor, P. Warzanowski, and T. Lorenz, Phys. Rev. B **90**, 104419 (2014).
- [41] B. Grenier, S. Petit, V. Simonet, L.-P. Regnault, E. Canévet, S. Raymond, B. Canals, C. Berthier, P. Lejay, arXiv: 1407.0213 (2014).
- [42] N. Shannon, B. Schmidt, K. Penc, and P. Thalmeier, Eur. Phys. J. B **38**, 599 (2004).
- [43] M. Horvatić and C. Berthier, "NMR Studies of Low-Dimensional Quantum Antiferromagnets," in C. Berthier, L. P. Levy, and G. Martinez, *High Magnetic Fields: Applications in Condensed Matter Physics and Spectroscopy* (Springer-Verlag, Berlin, 2002), p. 200.
- [44] D. Beeman and P. Pincus, Phys. Rev. **166**, 359 (1968).
- [45] R. Blinc, Phys. Rep. **79**, 331 (1981).
- [46] M. Klanjšek, (unpublished).
- [47] S. Suga, J. Phys. Soc. Jpn. **77**, 074717 (2008).
- [48] T. Hikihara and A. Furusaki, Phys. Rev. B **69**, 064427 (2004).
- [49] K. W. Plumb, K. Hwang, Y. Qiu, L. W. Harriger, G. E. Granroth, G. J. Shu, F. C. Chou, Ch. Rüegg, Y. B. Kim, Y.-J. Kim, arXiv: 1408.2528 (2014).
- [50] A. A. Tsirlin, I. Rousochatzakis, D. Kasinathan, O. Janson, R. Nath, F. Weickert, C. Geibel, A. M. Läuchli, and H. Rosner, Phys. Rev. B **82**, 144426 (2010).
- [51] Y. Kohama, S. Wang, A. Uchida, K. Prsa, S. Zvyagin, Yu. Skourski, R. D. McDonald, L. Balicas, H. M. Rønnow, Ch. Rüegg, and M. Jaime, Phys. Rev. Lett. **109**, 167204 (2012).